Analysis of Thomson Scattering from Nonequilibrium Plasmas

D. A. Chapman[1,2] and D. O. Gericke[1]

[1]Centre for Fusion, Space and Astrophysics, Department of Physics, University of Warwick, Coventry CV4 7AL, United Kingdom
[2]Plasma Physics Department, AWE plc, Aldermaston, Reading RG7 4PR, United Kingdom

(Received 19 April 2011; published 12 October 2011)

We develop the theory for light scattering as a diagnostic method for plasmas in nonequilibrium states. We show how well-known nonequilibrium features, like beam acoustic modes, arise in the spectra. The analysis of an experiment with strongly driven electrons demonstrates the abilities of the new approach; we find qualitatively different scattering spectra for different times and excellent agreement with the experimental data after time integration. Finally, an analysis of data from dense beryllium suggests that an energetic electron component exists in this experiment as well.

DOI: 10.1103/PhysRevLett.107.165004 PACS numbers: 52.70.−m, 52.59.Hq

Thomson scattering (TS) is a versatile technique that has become an indispensable diagnostic tool for a wide range of plasma physics experiments [1–4]. By measuring the spectrum of radiation scattered by the sample under study, the dielectric response of the electronic subsystem can be directly interrogated. Depending on the scattering geometry, such data are related to collective excitations or the thermal motion of the electrons, i.e., plasmons or the distribution function [5]. Fitting calculated spectra to measurements thus allows the basic plasma conditions to be inferred. The measured spectra may also be used to constrain or validate theoretical models for important macroscopic properties such as the electrical and thermal conductivities [6,7], and the equation of state [8–11].

The flux of radiation scattered from a sample is directly proportional to the dynamic structure factor (DSF) of the electrons $S_{ee}(\mathbf{q}, \omega)$ which contains all information on the microscopic electron correlations in space and time. In general, the calculation of the DSF requires a quantum statistical description of the fully coupled many-particle system including self-consistent dynamic screening of all the interactions [12]. However, it has been shown that the scattering spectrum can be approximately decomposed into contributions due to the high-frequency fluctuations of the free electrons, the low-frequency fluctuations of the electrons which dynamically follow the ion motion, and a contribution from inelastic Raman-like transitions [13]. Since the low-frequency fluctuations due to the ion motion cannot be resolved in many experiments [14], we focus on the inelastic feature in the scattering spectrum due to the (collective) motion of the free electrons. This part can often be described as an electron gas [13].

The DSF of the free electrons may be described within a one component plasma (OCP) model. To go beyond the standard description of the random phase approximation (RPA), much work has been undertaken to incorporate nonideality effects and collisions with the ions (see, e.g., Refs. [12,15]). However, current theoretical descriptions of the DSF require the electrons to be in thermodynamic equilibrium, i.e., to have a Fermi distribution with a well-defined temperature T_e. In this case, the DSF is related to the linear density response function, $\chi_{ee}(\mathbf{q}, \omega)$, by a fluctuation-dissipation theorem (FDT) of the form

$$S_{ee}(\mathbf{q}, \omega) = \frac{\hbar}{\pi n_e} \frac{1}{1 - \exp(-\beta_e \hbar \omega)} \Im\mathrm{m} \chi_{ee}(\mathbf{q}, \omega), \quad (1)$$

where $\beta_e = 1/k_B T_e$ is the inverse thermal energy. The use of this relation inherently restricts applications of TS to systems in thermal equilibrium and, thus, excludes many experiments of interest. In particular, Eq. (1) is invalid for measurements within the relaxation time after creation or if the system is driven, either externally or by the probe, during the measurement. Previously such effects have been considered for dilute plasmas probed with optical lasers only [16].

In this Letter, we develop the theory for the application of TS as a diagnostic method for dense, partially ionized systems in states far from equilibrium. Being based on quantum statistical theory, the new approach can also be applied to dense matter with degenerate electrons. Its application to an experiment using an intense VUV pulse for heating and probing [17] reveals the strong influence of nonequilibrium states on the scattering spectra which are thus strongly time dependent. Our analysis also shows that a small fraction of high-energy electrons can significantly modify the blue wing in the x-ray scattering spectra of Ref. [18].

In order to extend the method of TS to nonequilibrium systems, one must abandon the use of the equilibrium FDT (1) and instead determine the DSF via

$$S_{ee}(\mathbf{q}, \omega) = \frac{i\hbar}{2\pi n_e} \frac{\Pi^{>}_{ee}(\mathbf{q}, \omega)}{|\varepsilon(\mathbf{q}, \omega)|^2} \overset{\mathrm{RPA}}{=} \frac{S^0_{ee}(\mathbf{q}, \omega)}{|\varepsilon^{\mathrm{RPA}}(\mathbf{q}, \omega)|^2}, \quad (2)$$

where $\Pi^{>}_{ee}(\mathbf{q}, \omega)$ is a special polarization function [12]. The second equality shows how the DSF in RPA can be constructed from the ideal, noninteracting DSF screened by the dielectric function. The noninteracting DSF can be easily obtained, e.g., by the method of nonequilibrium

 © 2011 American Physical Society

Green's functions. In this case, the noninteracting DSF is proportional to the product of two single-particle Green's functions, which gives in Fourier space

$$S^0_{ee}(\mathbf{q},\omega) = \frac{2\hbar}{n_e}\int \frac{d^3\mathbf{p}}{(2\pi\hbar)^3}\,\delta(E(\mathbf{p}+\mathbf{q}) - E(\mathbf{p}) - \hbar\omega) \times [1 - f_e(\mathbf{p}+\mathbf{q})] f_e(\mathbf{p}). \quad (3)$$

$f_e(\mathbf{p})$ is the electron distribution function, which is time dependent for nonequilibrium, and $E(\mathbf{p}) = p^2/2m_e$ is the kinetic energy. This form of the free-particle DSF may be qualitatively understood by considering the Feynman diagram for s-wave Compton scattering, averaging over the distribution of initial electron momenta, and finally including the Pauli exclusion principle via the blocking factor $[1 - f_e(\mathbf{p}+\mathbf{q})]$ for the outgoing states.

The dielectric function $\varepsilon(\mathbf{q},\omega)$ which is screening the polarization $\Pi^{>}_{ee}(\mathbf{q},\omega)$ in Eq. (2) is, in general, given in terms of the fully coupled density response function $\varepsilon^{-1}(\mathbf{q},\omega) = 1 + V_{ee}(q)\chi_{ee}(\mathbf{q},\omega)$. Although much progress has been made in recent years [15], a general solution for $\varepsilon(\mathbf{q},\omega)$ or $\chi_{ee}(\mathbf{q},\omega)$ is currently not available. However, electrons are often only weakly coupled. For low-density plasmas produced by laser ablation, the thermal energy usually exceeds the interaction strength. On the other hand, the Fermi energy often dominates the correlations in systems with degenerate electrons such as warm dense matter. In both cases, we thus may apply the RPA to describe the electron response. The dielectric function then has the form

$$\varepsilon^{\mathrm{RPA}}(\mathbf{q},\omega) = 1 - V_{ee}(q)\chi^0_e(\mathbf{q},\omega), \quad (4)$$

where $V_{ee}(q) = 4\pi\hbar^2e^2/q^2$ is the bare Coulomb potential between the electrons and $\chi^0_e(\mathbf{q},\omega)$ is the density response function of the noninteracting system

$$\chi^0_e(\mathbf{q},\omega) = 2\int \frac{d^3\mathbf{p}}{(2\pi\hbar)^3}\,\frac{f_e(\mathbf{p}+\mathbf{q}) - f_e(\mathbf{p})}{E(\mathbf{p}+\mathbf{q}) - E(\mathbf{p}) - \hbar\omega - i0}. \quad (5)$$

The nonequilibrium electron distribution determines both the ideal DSF (3) and the screening function (4). Thus, the power and spectrum of light scattered from the free electrons is also fully determined by this distribution. Naturally, we recover the FDT (1) if the relaxation has established Fermi distributions.

Although the approach presented here is applicable to any nonequilibrium situation, we now focus on typical perturbations that arise from the interaction of plasmas with strong laser fields or highly brilliant probe pulses as provided by free electron lasers [19,20]. The absorption of photons propagates electrons to energy states shifted by the photon energy. For high photon energies or high intensity allowing for multiphoton absorption, a high-energy bump is generated in the distribution. Ultrafast relaxation quickly populates a equilibriumlike branch that can be described by a hot temperature [17,21]. Other mechanisms that can result in a two-temperature distribution are parametric instabilities and nonthermal absorption during the laser-plasma interaction [22–24]. Thus, the following form for the nonequilibrium electron distribution captures many important aspects of laser-plasma experiments while retaining analytic properties

$$f_e(p) = A_c f_{\mathrm{eq}}(p, T_c) + A_h f_{\mathrm{eq}}(p, T_h) + A_b e^{-(p-p_0)^2/p_b^2}. \quad (6)$$

The first two terms are equilibrium distributions which describe partially equilibrated electrons. Usually, they represent the main electron population at T_c and a hot, Boltzmann-like tail characterized by T_h. The third term gives a Gaussian distribution of high-energy electrons at the bump energy $E_b = p_0^2/2m_e$. The parameter p_b defines the characteristic width of the bump. The partial density of each term is determined by the weight factors A_i. Because of its form we refer to the distribution (6) as the bump on hot tail (BOHT) model. Note that the weights and temperatures, as well as the shift and width of the bump, are time-dependent parameters.

A basic dynamic property of nonequilibrium systems that can be probed by TS is the dispersion relation of the collective electron modes (plasmons) [7,18]. Requiring $\Re\mathrm{e}\,\varepsilon(\mathbf{q},\omega) = 0$, one obtains in the long wavelength limit, i.e. $q \to 0$, a modified Bohm-Gross dispersion relation

$$\omega_{\mathrm{pl}}(q) = \omega_{\mathrm{pe}}\left[1 + \frac{q^2\langle E_e\rangle}{m_e\hbar^2\omega^2_{\mathrm{pe}}}\right]. \quad (7)$$

$\omega_{\mathrm{pe}} = (4\pi n_e e^2/m_e)^{1/2}$ is the plasma frequency and $\langle E_e\rangle$ denotes the mean kinetic energy of the electrons. Clearly, even small contributions from highly energetic, i.e., nonthermal, electrons can significantly increase the plasmon frequency in this limit.

The example for the full plasmon dispersion in Fig. 1 shows that the nonequilibrium effects are in fact more complex for larger values of q. Adding a bump gives rise to a feature known as beam acoustic mode (BAM) which has quasilinear dispersion and couples strongly to the plasmon branch. BAMs have been studied analytically [25] and were recently observed experimentally [26,27]. For $q > 0.25\hbar/a_B$, the dispersion is dominated by the bulk electrons which are cold and Fermi-like in this case. Note that the low-frequency acoustic branch is unaffected by nonequilibrium parts of the distribution.

We now apply our analysis to recent experimental data obtained at the free electron laser FLASH at DESY in Hamburg [17]. Here, liquid (cryogenic) hydrogen was heated and probed for 40 fs by an intense pulse of VUV radiation. The high flux of 91.8 eV photons continuously photoionizes the hydrogen. Although the plasma is only weakly ionized, the relatively low atomic density prevents collisional damping to be significant thus justifying the use of the RPA response. Because of the high photon flux the

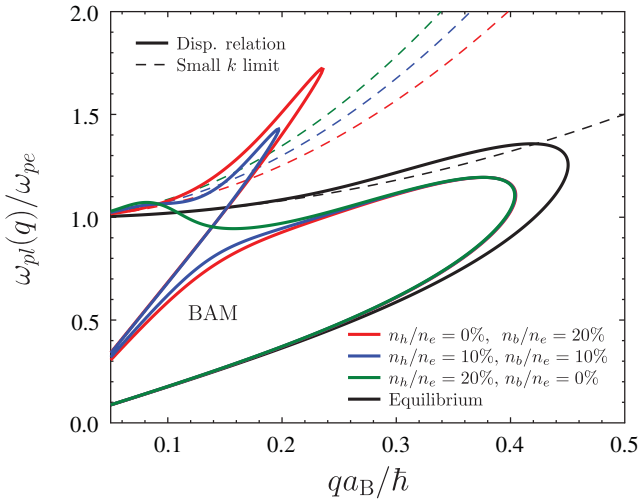

FIG. 1 (color). Plasmon dispersion for fully ionized liquid hydrogen ($n_e = 4.2 \times 10^{22}$ cm^{-3}) and different ratios of hot and cold electrons ($T_c = 2$ eV, $T_h = 50$ eV, $E_b = 50$ eV). The results of the small q expansion (dashed) are shown for comparison.

electrons are driven into highly nonequilibrium states by populating energies with $E_b = \hbar\omega - E_{\text{ion}} = 77.6$–$78.2$ eV. Scattering processes then lead to the filling of states with lower energies and finally thermalization.

Cluster simulations were used to quantify this picture (see Ref. [17]). The distributions obtained can, indeed, be approximated by the BOHT model as shown in Fig. 2(a). In particular, the simulations show that the bump quickly diffuses into a hot tail, as expected, while the bulk of the electrons experience minimal heating due to the large difference in energy scales. On the other hand, a Fermi distribution does not fit the simulation results at any time throughout the pulse.

As the BOHT model fits the cluster simulations quite well, we will base our analysis of the scattering spectrum on this form. Figure 2(b) compares the DSFs calculated from Eq. (2) for the 3 times/distributions of Fig. 2(a) with the equilibrium DSF using conditions reported in Ref. [17]. At early times the scattering is noncollective as the free electron density is very low. For these times the spectrum reflects the shape of the distribution function [5] where the large steplike wings are the result of the bump. The development of well-defined, plasmonlike peaks in the spectrum and the diminishing contributions from the high-energy electrons can be seen from the peak of the pulse onwards when the ionization increases and the distribution equilibrates. At late times the plasmon is noticeably upshifted relative to the best equilibrium fit, suggesting that the final free electron density may be underestimated using an equilibrium analysis.

To compare to the experimental data, we compute the scattered power spectra for the evolving system and then integrate over the probe duration as the measurement was time integrated. Figure 2(c) shows that this procedure yields excellent agreement between the calculated and measured spectra although the latter does not represent any of the instantaneous power spectra. Time-averaging nonequilibrium calculations also gives an improved fit to the redshifted plasmon and to the wings of the spectrum, where the equilibrium approach fits less well. The elastic scattering from bound electrons is negligible here as the ions retain the liquid structure over fs time scales [28].

The ratio of the red- and blueshifted peaks (detailed balance for equilibrium systems) is also in agreement

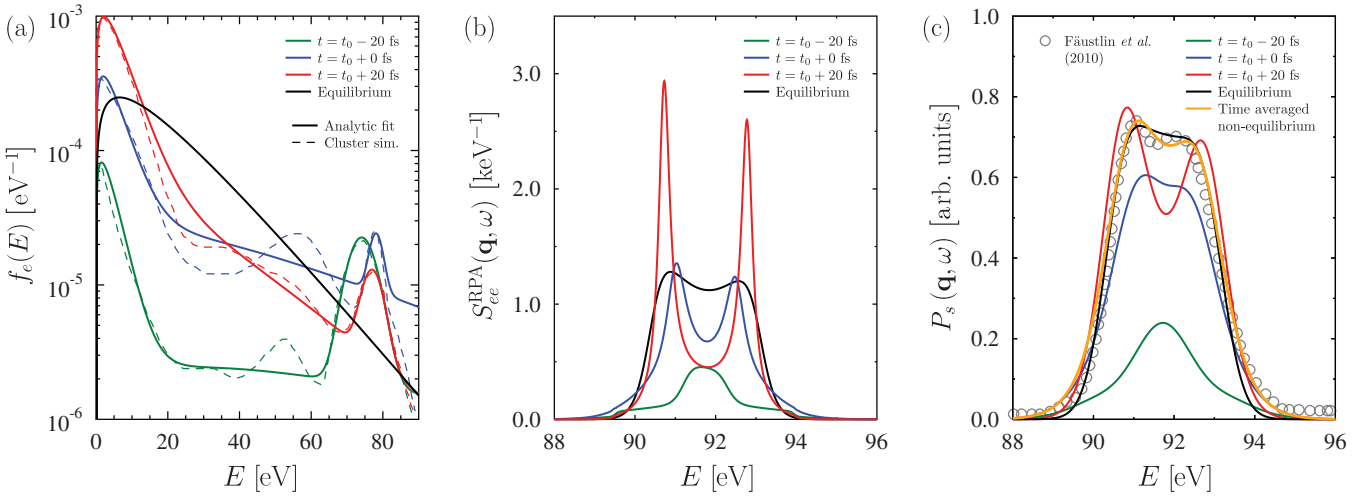

FIG. 2 (color). (a) Fits to the time-resolved distribution function from Ref. [17] using the BOHT model (6); t_0 labels the time at the peak of the pulse. For comparison, a Fermi function with electron density and temperature as obtained by fitting the spectra to an equilibrium calculation ($n_e = 2.8 \times 10^{20}$ cm^{-3} and $T_e = 13$ eV) is shown. (b) Dynamic structure factors (2) following from the distributions in panel (a). (c) Scattered power spectra convolved with the spectrum of the VUV source for the same 3 times, and a time-integrated spectrum compared to both the experimental data [17] and the best fit equilibrium calculation.

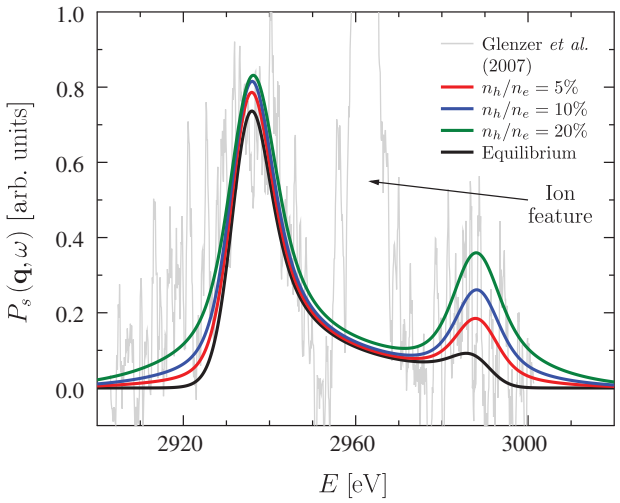

FIG. 3 (color). Effect of a hot tail with $T_h = 100$ eV on the spectrum of isochorically heated beryllium with a bulk temperature of $T_c = 12$ eV and a total electron density of $n_e = 2.46 \times 10^{23}$ cm^{-3} compared to experimental data from Ref. [18].

with both the data and the equilibrium best fit with $T = 13$ eV, despite the fact that the majority of the electrons are at a much lower temperature ~4 eV. This can be understood by calculating the (time-averaged) mean kinetic energy, which is ~13 eV. The temperature of the best fit in the equilibrium model thus reflects this energy scale.

The fact that the experimental scattering spectrum is well-represented by calculations based on fundamentally different electron distributions needs further discussion as it may support conflicting conclusions on the microscopic dynamics of the system, e.g., relaxation rates. This result occurs mainly due to cancellations of features during the time averaging. Moreover, while the time-averaged mean energy and density are similar in both calculations, the final bulk temperature and electron density are larger by factors of ~3 and ~2, respectively. These errors, which are introduced by assuming equilibrium conditions, are significant for any subsequent measurements of dynamic or thermodynamic properties of the system.

Nonequilibrium physics may also help to elucidate the difficulties in the interpretation of scattering data from heated, solid-density beryllium [18]. In this experiment, the heating is sufficiently slow (~ 1 ns) for the majority of the electrons to be thermalized, although a small weight, hot tail generated by the x-ray pump may still persist. Taking the plasma conditions reported and considering a hot tail ($T_h = 100$ eV) strongly improves the agreement between theory and experiment on the blueshifted side of the spectrum (see Fig. 3). The figure also demonstrates that only a small fraction of hot electrons, i.e., 5%–10%, is sufficient to explain the large scatter at the blueshifted plasmon, which is strongly underestimated by calculations based on an equilibrium model. Interestingly, the redshifted plasmon is almost unaffected.

The wings of the spectrum are also enhanced in the direction of the data where an increase of T_h extends the wings further and lowers the relative density of the hot tail necessary to match the balance between the red- and blueshifted plasmons. Moreover, including a hot tail also gives rise to wings on the Compton feature when probing via noncollective scattering as in Ref. [29]. Consequently, it reduces the ionization, which is inferred by comparing the amplitudes of the Compton and Rayleigh features, and brings it closer to the theoretical prediction of $Z = 2$. As a population of hot electrons also gives rise to higher charge states, due to enhanced impact ionization, the remaining discrepancy might be further mitigated.

In conclusion, we have developed a theory for Thomson scattering applicable to plasmas in which the electrons are driven into states that are far from equilibrium. We assessed the impact of nonequilibrium distributions on the interpretation of experimental scattering data for a classical plasma and warm dense matter with degenerate electrons. For strongly driven hydrogen probed on ultrashort time scales, we find large variations of the predicted spectra with time and excellent agreement with measured data after time integration. For warm dense beryllium, it was shown that only a small fraction of hot electrons may have a significant effect on the predicted spectra and yield a better agreement with experimental measurements.

The authors thank M. Schlanges (Univ. Greifswald) for fruitful discussions and EPSRC for financial support.

[1] N. J. Peacock *et al.*, Nature (London) **224**, 488 (1969).
[2] S. H. Glenzer *et al.*, Phys. Plasmas **6**, 2117 (1999).
[3] O. L. Landen *et al.*, J. Quant. Spectrosc. Radiat. Transfer **71**, 465 (2001).
[4] G. Gregori *et al.*, Phys. Rev. E **67**, 026412 (2003).
[5] S. H. Glenzer and R. Redmer, Rev. Mod. Phys. **81**, 1625 (2009).
[6] J. L. Kline *et al.*, JINST **5**, P11005 (2010).
[7] P. Neumayer *et al.*, Phys. Rev. Lett. **105**, 075003 (2010).
[8] A. L. Kritcher *et al.*, Phys. Rev. Lett. **103**, 245004 (2009).
[9] S. Le Pape *et al.*, Phys. Plasmas **17**, 056309 (2010).
[10] A. Pelka *et al.*, Phys. Rev. Lett. **105**, 265701 (2010).
[11] H. J. Lee *et al.*, Phys. Rev. Lett. **102**, 115001 (2009).
[12] D. Kremp, M. Schlanges, and W.-D. Kraeft, *Quantum Statistics of Nonideal Plasmas* (Springer, Berlin, 2006).
[13] J. Chihara, J. Phys. F **17**, 295 (1987).
[14] G. Gregori and D. O. Gericke, Phys. Plasmas **16**, 056306 (2009).
[15] C. Fortmann, A. Wierling, and G. Ropke, Phys. Rev. E **81**, 026405 (2010).
[16] E. Fourkal *et al.*, Phys. Plasmas **8**, 550 (2001).
[17] R. R. Fäustlin *et al.*, Phys. Rev. Lett. **104**, 125002 (2010).
[18] S. H. Glenzer *et al.*, Phys. Rev. Lett. **98**, 065002 (2007).
[19] W. Ackermann *et al.*, Nat. Photon. **1**, 336 (2007).
[20] P. Emma *et al.*, Nat. Photon. **4**, 641 (2010).

[21] N. Medvedev *et al.*, Phys. Rev. Lett. **107**, 165003 (2011)
[22] W. L. Kruer, *The Physics of Laser-Plasma Interactions* (Westview, Boulder, 2003).
[23] S. C. Wilks *et al.*, Phys. Rev. Lett. **69**, 1383 (1992).
[24] F. N. Beg *et al.*, Phys. Plasmas **4**, 447 (1997).
[25] T. M. O'Neil and J. H. Malmberg, Phys. Fluids **11**, 1754 (1968).
[26] J. L. Kline *et al.*, Phys. Rev. Lett. **94**, 175003 (2005).
[27] H. X. Vu *et al.*, Phys. Rev. Lett. **95**, 245003 (2005).
[28] D. A. Chapman *et al.* [HEDP (to be published)].
[29] S. H. Glenzer *et al.*, Phys. Rev. Lett. **90**, 175002 (2003).